Virtual Array Processing for Active Radar and Sonar Sensing

Louis L. Scharf and Ali Pezeshki

***Abstract*— In this paper, we describe how an active radar/sonar imaging problem may be formulated as a virtual passive sensor array processing problem. We consider an active sensing problem where it is desired to form a range-Doppler image at a slow-time rate, even though the radar/sonar can transmit pulses at a fast time rate. By transmitting pulses at the fast time rate we can estimate the second-order statistics of an ambiguity vector, calculated at a coarse resolution. As we show this ambiguity vector plays the role of an array snapshot vector in passive sensor array processing. The noise free version of this ambiguity vector acts as a signature vector or steering vector, which can be steered around in delay and Doppler at a fine resolution to produce an image. We employ a MVDR-like principle to generate high resolution delay-Doppler images.**

I. Introduction

Consider an active radar/sonar sensing problem, where it is desired to estimate the target range and Doppler every t_s seconds, even though the radar can transmit pulses at rate $\frac{1}{t_f} = \frac{K}{t_s}$, $K >> 1$ during each interval $t_s = Kt_f$. In other words, there are two time scales: a fast-time t_f, which determines the pulse repetition rate and a slow-time $t_s = Kt_f$, which determines the rate at which the range-Doppler map is updated. This two time-scale idea is illustrated in Fig. 1, where K waveforms, each with time-bandwidth product $2TW$, are transmitted during a slow-time interval t_s.

By transmitting pulses at the fast rate we estimate second-order statistics of an ambiguity vector, whose elements are samples of the ambiguity function between the radar data and the transmit pulse, at resolution $1/2W$ in range and $1/T$. This ambiguity vector may be viewed as a virtual array snapshot vector that samples the ambiguity function in delay and Doppler, just like the way an actual sensor array samples a wavefront in space. This analogy allows us to convert an active radar/sonar imaging problem into a virtual passive sensor array processing problem. We show how standard beamforming techniques like minimum variance distortionless response (MVDR) beamforming can be employed in our virtual array processing problem to generate high resolution range and Doppler images.

II. Virtual Array Processing for Active Sensing

A. Range-Doppler Processing

Let $u(t)$ be a transmit waveform with time-bandwidth product $2TW$ (time-limited to $[0, T)$ and band-limited to $(-W, W]$) and $y(t)$ be the received signal. Tessellate the ambiguity region into L cells centered at $(n/2W, m/T)$ for $n = 0, 1, \ldots, N-1$ and $m = 0, 1, \ldots, M-1$, with $L = NM$. The complex baseband output of an imaging radar/sonar for the (n, m)th cell, centered at $(n/2W, m/T)$, will be the correlation (cross-ambiguity)

$$\begin{aligned} y_{nm} &= \langle y(t), M_{m/T} T_{n/2W} u(t) \rangle \\ &= \int y(t) u^\star(t - \tfrac{n}{2W}) e^{-j2\pi \frac{m}{T} t} dt, \end{aligned} \tag{1}$$

where $T_{n/2W}$ is the delay operator by $n/2W$, $M_{m/T}$ is the modulation operator at Doppler frequency $2\pi m/T$, and $\langle \, , \, \rangle$ is the inner product between two complex energy signals. For now we assume that each received signal may be imaged in both range and Doppler, as in (1), to estimate a coarse-grained ambiguity function. Later on in Section II-B, we generalize our development to the case where the ambiguity surface is poorly resolved in Doppler due to the small time-bandwidth product of the transmit pulse, in which case Doppler imaging has to be performed by taking the FFT of the range-only imaged returns from a sequence of pulses.

If we organize the L values of y_{nm}, $n = 0, \ldots, N-1$, $m = 0, \ldots M-1$, with $L = MN$, into a vector $\mathbf{y} = [y_0, \ldots, y_{L-1}]^T \in \mathbb{C}^L$, we may look at $\mathbf{y}$ as a "virtual" L-element sensor array snapshot with covariance $\mathbf{R} = E[\mathbf{y}\mathbf{y}^H]$. The virtual sensor array we have built here samples the radar ambiguity function at delay intervals $1/2W$ and Doppler intervals $1/T$, just like an actual array snapshot vector samples of the phase and amplitude functions of a propagating wavefront at half-wavelength intervals in space.

Assuming that the target of interest is a point target located at cell $(0, 0)$, and that it is uncorrelated with the clutter and noise, the target gain g and the vector $\mathbf{y} = \mathbf{r}g + \mathbf{n}$ share a composite covariance matrix of the form

$$E \begin{bmatrix} g \\ \mathbf{y} \end{bmatrix} \begin{bmatrix} g^\star & \mathbf{y}^H \end{bmatrix} = \begin{bmatrix} \sigma_g^2 & \mathbf{r}^H \\ \mathbf{r} & \mathbf{R} \end{bmatrix}. \tag{2}$$

The cross-correlation vector $\mathbf{r} = E[\mathbf{y}g^\star]$ is the ambiguity function for the transmitted signal, at delay zero and modulation zero (with respect to the center of the ambiguity region). Its ith element is the ambiguity at cell i, corresponding to some pair (n, m). The cross-correlation vector (waveform ambiguity vector) $\mathbf{r}$, which determines the range-Doppler signature of target g, plays the role of a steering (direction) vector in the virtual array processing problem. The measurement covariance matrix $\mathbf{R} = \sigma_g^2 \mathbf{r}\mathbf{r}^H + \mathbf{R}_0$, with $\mathbf{R}_0$ the covariance of clutter plus noise, is in general unknown. However, $\mathbf{R}$ may be estimated, if during a slow-time interval the waveform $u(t)$ is transmitted several times, yielding a sequence of K realizations of $\mathbf{y}$:

$$\hat{\mathbf{R}} = \frac{1}{K} \sum_{k=1}^{K} \mathbf{y}[k] \mathbf{y}^H[k]. \tag{3}$$

L. L. Scharf is with the Departments of Electrical and Computer Engineering, and Statistics, Colorado State University, Fort Collins, CO 80523-1373, USA, Phone: (970) 491-2979, Fax: (970) 491-2249 (e-mail:scharf@engr.colostate.edu).

A. Pezeshki is with The Program in Applied and Computational Mathematics, Princeton University, Princeton, NJ 08544-1000, USA, Phone: (609) 258-5784, Fax: (609) 258-1735 (email: pezeshki@princeton.edu).

This work is supported in part under DARPA contracts FA9550-04-1-0371 and FA8750-05-2-0285, and ONR contract N00014-04-1-0084.

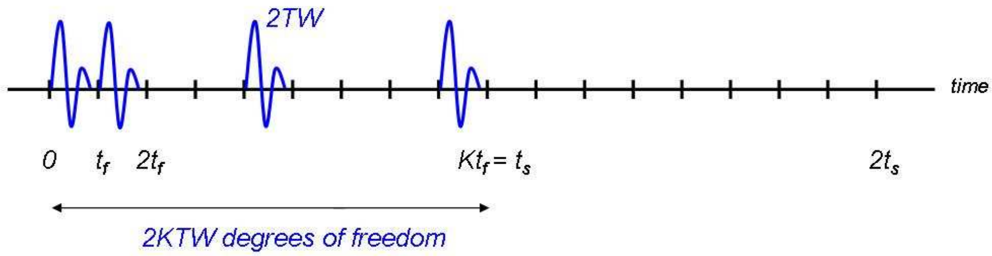

Fig. 1. The two-time scale idea

This argument shows that active range-Doppler imaging of a point target in clutter and noise may be viewed as a virtual passive sensor array processing problem, in which a sequence of virtual wavefronts with direction vectors $\mathbf{r}$ are incident on the array, producing snapshot vectors $\mathbf{y}[1], \ldots, \mathbf{y}[K]$ with experimental covariance $\hat{\mathbf{R}}$. In Section III, we shall discuss how this array processing formulation can be used to form a high resolution radar image.

B. Doppler Processing

The arguments in the previous section assume that each pulse return can be imaged in both range and Doppler. In a radar system where the time-bandwidth product $2TW$ of the transmit waveform is small, the ambiguity surface is poorly resolved in Doppler, and hence is not useful for Doppler imaging. Our aim in this section is to show that the formulation of Section II-A may be easily modified to allow for Doppler imaging in such scenarios.

Suppose we only image the received signal $y(t)$ in range, by matching it to the transmit waveform $u(t)$ at N different range cells at resolution $1/2W$, to get the matched filter outputs x_n:

$$\begin{aligned} x_n &= \langle y(t), T_{n/2W} u(t) \rangle \\ &= \int y(t) u^\star(t - \tfrac{n}{2W}) dt; \quad n = 0, 1, \ldots, N-1. \end{aligned} \tag{4}$$

Suppose the waveform $u(t)$ is transmitted M times, resulting in M copies of each matched filter output x_n. Then, we can arrange these matched filter outputs in an $N \times M$ matrix $\mathbf{X}$ as

$$\begin{aligned} \mathbf{X} &= \begin{bmatrix} x_0[0] & x_0[1] & \cdots & x_0[M-1] \\ x_1[0] & x_1[1] & \cdots & x_1[M-1] \\ \vdots & & & \vdots \\ x_{N-1}[0] & x_{N-1}[1] & \cdots & x_{N-1}[M-1] \end{bmatrix} \\ &= \begin{bmatrix} \mathbf{x}_0^T \\ \mathbf{x}_1^T \\ \vdots \\ \mathbf{x}_{N-1}^T \end{bmatrix}, \end{aligned} \tag{5}$$

where $x_n[m]$ is the matched filter output corresponding to the the nth range cell and the mth waveform transmission. Therefore, the nth row of $\mathbf{X}$, i.e., $\mathbf{x}_n^T = [x_n[0], \ldots, x_n[M-1]]$, carries the M matched filter outputs obtained by range imaging at the nth range cell. Note that

$$x_n[m] = x_n[0] e^{jm\theta}, \quad m = 0, \ldots, M-1, \tag{6}$$

where $\theta = 2\pi \frac{v}{C} f_0 t_f$ is the phase difference between two consecutive pulses due to Doppler, f_0 is the carrier frequency, v is the speed of the target, and C is the speed of light. If the maximum target speed to be covered by the radar is $v_{max} = V$, then we must have

$$\theta = 2\pi \frac{V}{C} f_0 t_f \leq 2\pi \tag{7}$$

or alternatively

$$\frac{1}{t_f} \geq \frac{V}{C} f_0. \tag{8}$$

This means that the pulse repetition frequency of the radar must not be smaller than the maximum Doppler frequency to be covered.

Doppler imaging may be achieved by post-multiplying $\mathbf{X}$ by the M-point FFT matrix $\mathbf{F}$:

$$\mathbf{Z} = \begin{bmatrix} \mathbf{z}_0^T \\ \vdots \\ \mathbf{z}_{N-1}^T \end{bmatrix} = \mathbf{X}\mathbf{F}; \quad \mathbf{F} = \{e^{j\frac{2\pi}{M}mn}\}_{mn}. \tag{9}$$

This way the Doppler band supported by the PRF of the radar is resolved into M Dopplers $\frac{V}{M}m$, without aliasing. The matrix $\mathbf{Z}$ contains $L = MN$ values obtained by processing the received signal $y(t)$ at N points in range and M points in Doppler. If we now organize these L values in a vector $\mathbf{z}$ of the form $\mathbf{z} = [\mathbf{z}_0^T, \ldots, \mathbf{z}_{N-1}^T]^T \in \mathbb{C}^L$ we obtain a “virtual” L-element array snapshot vector of range-Doppler maps, similar to that in Section II-A.

To obtain K' multiple realizations of the array snapshot vector $\mathbf{z}$, the waveform $u(t)$ has to be transmitted $K'M$ times. Each time a waveform is transmitted we image the received signal in range-only at the coarse resolution $1/2W$. After a series of M such imagings we Doppler image at each range cell and vectorize the resulting range-Doppler images to obtain a new copy (a new realization) of the array snapshot vector $\mathbf{z}$. We may then use these copies to estimate the array covariance matrix $\mathbf{R}$ as in (3). However, instead of $K = K'M$ realizations, we can have at most K' realizations of $\mathbf{z}$ to estimate the covariance matrix $\mathbf{R}$. This shows that as usual there is a tradeoff between bias and variance, with bias in this case corresponding to the Doppler resolution for the ambiguity surface, which is determined by M, and variance corresponding to the statistical variability of the ambiguity surface. In summary, K re-transmissions of a waveform with time-bandwidth product $2TW$ offers $2KTW$

degrees of freedom. If $2MTW$ of these degrees are used for range-Doppler imaging, then just $K' = K/M$ degrees of freedom remain for averaging to estimate $\mathbf{R}$.

Similar to the previous section, the steering vector or the cross-correlation vector $\mathbf{r}(n,m)$ in this case is a vector of ambiguity values at different range-Doppler cells. The only difference is that this time the ambiguity values are computed at Doppler frequencies that are specified by the M-point FFT, which is performed for Doppler imaging at each range.

III. MVDR-like Radar Imaging

In standard MVDR beamforming, the beamformer vector $\mathbf{w} \in \mathbb{C}^L$ is designed to minimize the power $P = E[|\mathbf{w}^H\mathbf{y}|^2] = \mathbf{w}^H\mathbf{R}\mathbf{w}$ at the output of the beamformer, with $\mathbf{R}$ the array measurement covariance matrix, under the constraint that the beamformer produces a distortionless response to the normalized steering vector $\mathbf{r}$:

$$\min_{\mathbf{w}} \mathbf{w}^H\mathbf{R}\mathbf{w} \quad \text{subject to} \quad \mathbf{w}^H\mathbf{r} = 1. \tag{10}$$

Often $\mathbf{r}$ is parameterized by a single variable like arrival angle as in $\mathbf{r} = [1, e^{j\theta}, \ldots, e^{j(L-1)\theta}]^T$, but this is not required. The minimization in (10) results in the MVDR beamformer $\mathbf{w}$ and minimum output power P of the form

$$\mathbf{w} = \frac{\mathbf{R}^{-1}\mathbf{r}}{\mathbf{r}^H\mathbf{R}^{-1}\mathbf{r}}, \tag{11}$$

$$P = \frac{1}{\mathbf{r}^H\mathbf{R}^{-1}\mathbf{r}}. \tag{12}$$

To generate an image the steering vector $\mathbf{r}$ is scanned in the parameter of $\mathbf{r}$ (for example angle θ) at a fine resolution, finer than the half-wavelength spacing. The parameter value at which the power peaks gives an estimate of the parameter of interest.

In our virtual array processing problem the steering vector $\mathbf{r}$ is parameterized by range and Doppler. It carries samples of the waveform ambiguity vector at delay intervals $1/2W$ and Doppler intervals $1/T$. To form an image we steer the waveform ambiguity vector $\mathbf{r}$ in range and Doppler at a fine resolution (τ_o, ν_o), where each $2TW$ cell contains multiple $\tau_o\nu_o$ cells, and calculate the output power P for each $\tau_o\nu_o$ cell. Letting $\mathbf{r}(n', m')$ denote the waveform ambiguity vector $\mathbf{r}$ when it is steered to cell $(n'\tau_o, m'\nu_o)$ the elements of $\mathbf{r}(n'\tau_o, m'\nu_o)$ are samples of the waveform ambiguity function at delay intervals $1/2W$ and Doppler intervals $1/T$, after the ambiguity function is shifted in delay by $n'\tau_o$ and modulated in Doppler by $m'\nu_o$. In other words, $\mathbf{r}(n'\tau_o, m'\nu_o)$ is

$$\mathbf{r}(n', m') = \text{vec}\{\langle M_{m/T}T_{n/2W}u(t), M_{m'\nu_o}T_{n'\tau_o}u(t)\rangle\}. \tag{13}$$

This is analogous to the standard passive sensor array processing, in which we steer the direction vector around in angle at a fine resolution but the array still samples the wavefront in space at half-wavelength intervals.

The output power P, when steering to $(n'\tau_o, m'\nu_o)$, is given by

$$P(n', m') = \frac{1}{\mathbf{r}^H(n', m')\hat{\mathbf{R}}^{-1}\mathbf{r}(n', m')}. \tag{14}$$

The output power P estimates the target power σ_g^2 when $\mathbf{r}(m', n')$ is steered to the center of the $\tau_o\nu_o$ cell in which the target lies.

Remark 1: In cases where the point target assumption made in writing the cross-correlation vector $\mathbf{r}$ is not trustworthy, we may assume that $\mathbf{r}$ lies in a known multi-dimensional subspace. Then $\mathbf{r}$ may be modelled as

$$\mathbf{r} = \mathbf{\Psi}\mathbf{b}, \tag{15}$$

where $\mathbf{\Psi} \in \mathbb{C}^L$ is a basis for a multi-dimensional subspace $\langle\mathbf{\Psi}\rangle$ and $\mathbf{b}$ is a vector of complex amplitudes. In many situations the subspace $\langle\mathbf{\Psi}\rangle$ will be a multi-dimensional Slepian-like subspace [1]-[3]. In distributed target scenarios, matched subspace detectors of [4],[5], adaptive subspace detectors and adaptive coherence estimators of [6],[7], matched direction detectors of [8], and multi-rank MVDR beamformers of [9], may be used to detect the target.

Remark 2: The virtual sensor array processing method described here can easily be extended to radar systems with multiple receive antennas. In such cases, we simply replace $\mathbf{r}$ with $\mathbf{r}' = \mathbf{r} \otimes \boldsymbol{\psi}(\theta) \in \mathbb{C}^{LL'}$, where $\boldsymbol{\psi}(\theta) \in \mathbb{C}^{L'}$ is the vector that carries the phases and amplitudes of the measurements at different receive elements, relative to the measurement at one of the receive elements, L' is the number of receive elements, θ is the angle of arrival of the radar echo, and $\otimes$ is the Kronecker product.

IV. Numerical Results

In this section, we present a numerical example to show how MVDR-like imaging can be used to form a high-resolution delay-Doppler image.

We consider a square ambiguity region of area $36/(2TW)$. We tessellate this ambiguity region into cells of size $1/2TW$ ($1/2W$ in delay and $1/T$ in Doppler). We use a chirp signal with $2TW = 16$ as the transmit pulse. Each time a pulse is transmitted we generate a received signal using the discretized measurement equation

$$y(lt_0) = \sum_i u(lt_0 - \tau_i)e^{j2\pi\nu_i lt_0}g_i + n(lt_0), \tag{16}$$

where τ_i and ν_i are delay and Doppler coordinates of the ith point target in the ambiguity region and g_i is the corresponding target gain with $E[g_i g_i^*] = \sigma_{g_i}^2$, and $1/t_0$ is an appropriate sampling rate.

After generating the measurement time-series $\{y(lt_0)\}$ we calculate the correlations y_{nm}, by approximating the integral in (1) by

$$\begin{aligned} y_{nm} &= \int y(t)u^\star(t - \tfrac{n}{2W})e^{-j2\pi\frac{m}{T}t}dt \\ &\approx \sum_l y(lt_0)u^\star(lt_0 - \tfrac{n}{2W})e^{-j2\pi\frac{m}{T}lt_0}. \end{aligned} \tag{17}$$

The sampling rate $1/t_0$ must be selected so that it allows for shifting the waveform $u(t)$ to target delay coordinates τ_i.

The calculation in (17) is done for every $1/2TW$ cell within the ambiguity region, resulting in $L = 36$ ambiguity samples ($N = 6$ and $M = 6$). Finally by vectorizing these ambiguity samples we obtain a realization of the L-dimensional virtual array snapshot vector $\mathbf{y}$. We re-transmit the waveform $u(t)$ and repeat the above procedure over and over again to obtain multiple realizations of $\mathbf{y}$ and subsequently estimate the array

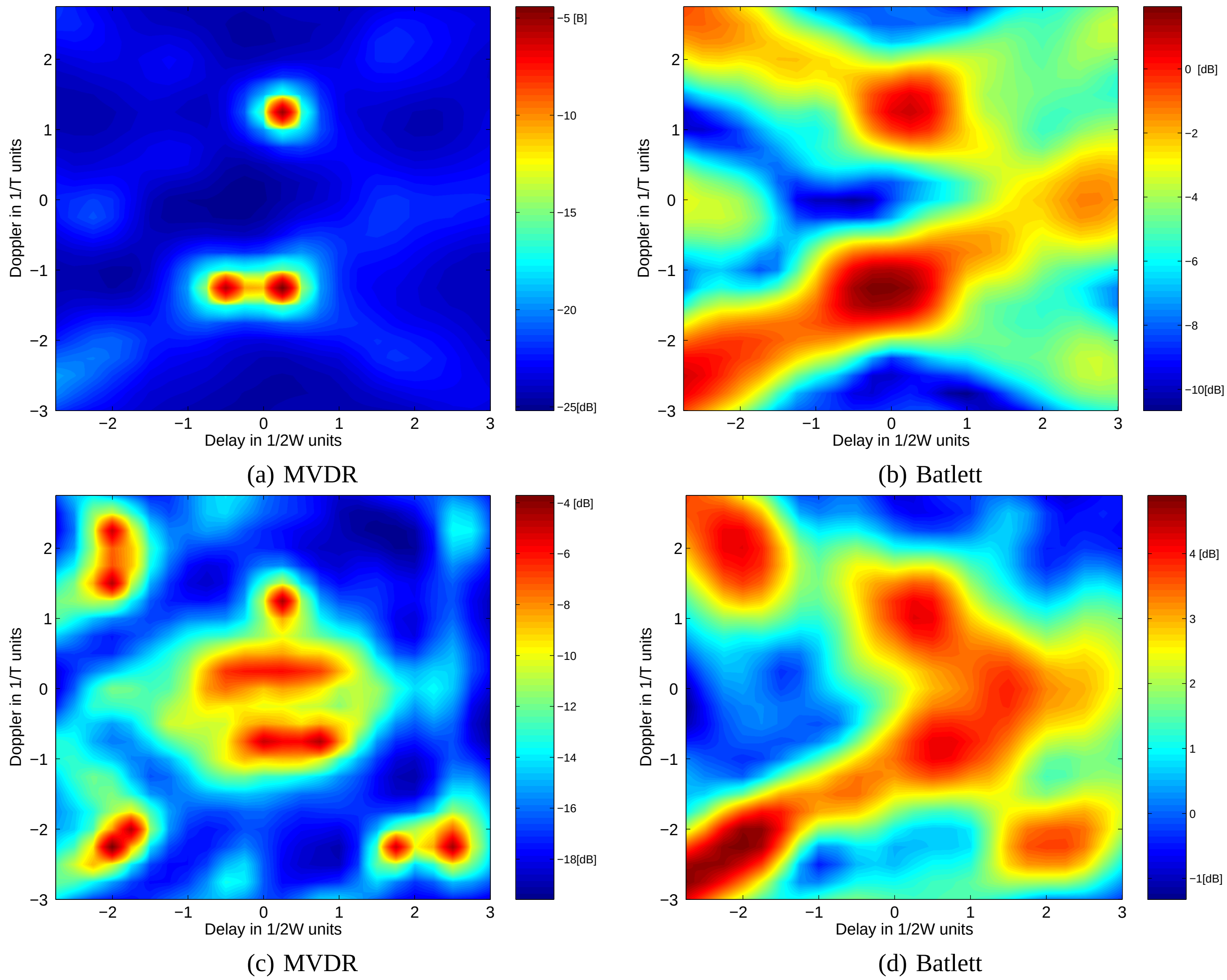

(a) MVDR (b) Batlett

(c) MVDR (d) Batlett

Fig. 2. Range-Doppler images obtained using MVDR imaging and Bartlett beamforming.

covariance matrix $\mathbf{R}$ as in (3). Here we estimate $\mathbf{R}$ using $K = 50$ transmissions.

To form the range-Doppler image we scan the ambiguity vector $\mathbf{r}(n', m')$ with resolution $\tau_o = 1/(4 \times 2W)$ in delay and $\nu_o = 1/4T$ in Doppler:

$$\begin{aligned} \mathbf{r}(n'\tau_o, m'\nu_o) &= \text{vec}\{\langle M_{m/T} T_{n/2W} u(t), M_{m'\nu_0} T_{n'\tau_0} u(t)\rangle\} \\ &\approx \text{vec}\{\sum_l u(lt_0 - \tfrac{n}{2W}) u^*(lt_0 - n'\tau_0) e^{-j2\pi(m'\nu_o - \frac{m}{T})lt_0}\} \end{aligned} \quad (18)$$

and calculate the power $P(n', m')$ in (14) for each $\tau_o\nu_o$ cell.

We compare MVDR-like imaging with conventional (Bartlett) beamforming, whose output power at cell $(n'\tau_o, m'\nu_o)$ is given by

$$P_B(n', m') = \mathbf{r}(n', m')^H \mathbf{R} \mathbf{r}(n', m'). \quad (19)$$

For the first example we place three point targets at delay and Doppler coordinates $(\tau_1 = \tau_o, \nu_1 = 6\nu_o)$, $(\tau_1 = -2\tau_o, \nu_1 = -4\nu_o)$, and $(\tau_1 = \tau_o, \nu_1 = -4\nu_o)$. The last two targets are placed closer than the classical range-Doppler resolution $1/2TW$. The signal-to-noise ratio (SNR) for each source is set to 4dB. The MVDR and Bartlett range-Doppler images are shown in Figs. 2(a),(b), respectively. We notice that the two point targets are not resolvable by the Bartlett beamformer, but they are resolved by the MVDR beamformer. This is analogous to the passive sensor array processing, where sources that are closer than the Rayleigh limit are not resolvable by the Bartlett beamformer, but they can be resolved by the MVDR beamformer.

We now consider an example with several point targets and clutter. We place nine point targets inside the ambiguity region at range-Doppler coordinates $(0, -2\nu_o)$, $(3\tau_o, -2\nu_o)$, $(\tau_o, 6\nu_o)$, $(7\tau_o, -8\nu_o)$, $(10\tau_o, -8\nu_o)$, $(-8\tau_o, 7\nu_o)$, $(-8\tau_o, 10\nu_o)$, $(-8\tau_o, -8\nu_o)$, and $(-7\tau_o, -7\nu_o)$. All the adjacent sources in range and Doppler are closer than the $1/2TW$ resolution. We also include a stationary (zero Doppler) clutter source that extends in range from $-\tau_o$ to τ_o. We set the SNR for each target to 4dB, and the signal-to-clutter ratio to -3dB. The MVDR and Bartlett range-Doppler images are shown in Figs. 2(c), (d), respectively. We notice that the Bartlett beamformer fails to resolve the sources. The MVDR beamformer on the other hand is able to resolve all the sources, even the ones near the clutter.

V. CONCLUSIONS

In summary, we have described how an active radar/sonar imaging problem can be formulated as a virtual passive sensor array processing problem. We have shown how standard MVDR beamforming can be employed to generate high resolution delay-Doppler images. Numerical examples were presented demonstrating the performance of MVDR-like imaging.

REFERENCES

[1] D. Slepian, "Prolate spheroidal wave functions, Fourier analysis and uncertainty - V: The discrete case," *Bell Syst. Tech. J.*, pp. 1371–1430, 1978.
[2] D. J. Thomson, "Spctrum estimation and harmonic analysis," *Proc. IEEE*, vol. 70, pp. 1055–1096, Sept. 1982.
[3] C. T. Mullis and L. L. Scharf, "Quadratic estimators of the power spectrum," in *Advances in Spectrum Estimation*, S. Haykin, Ed. Prentice Hall, 1990, vol. 1, ch. 1, pp. 1–57.
[4] L. L. Scharf, *Statistical Signal Processing*, pp. 330–331, Addison-Wesley, MA, 1991.
[5] L. L. Scharf and B. Friedlander, "Matched subspace detectors," *IEEE Trans. Signal Processing,* vol. 42, pp. 2146–2157, Aug. 1994.
[6] S. Kraut, L. L. Scharf, and L. T. McWhorter, "Adaptive subspace detectors," *IEEE Trans. Signal Processing,* vol. 49, pp. 1–16, Jan. 2001.
[7] S. Kraut, L. L. Scharf, and R. Butler, "The adaptive coherence estimator: a uniformly-most-powerful invariant apadtive detection statistics," *IEEE Trans. Signal Processing,* vol. 53, pp. 427–438, Feb. 2005.
[8] O. Besson, L. L. Scharf, and F. Vincent, "Matched direction detectors and estimators for array processing with subspace steering vector uncertainties," *IEEE Trans. Signal Processing,* vol. 53, pp. 4453–4463, Dec. 2005.
[9] A. Pezeshki, B. D. Van Veen, L. L. Scharf, H. Cox, and M. Lundberg, "Eigenvalue beamforming using a multi-rank MVDR beamformer and subspace selection," submitted to *IEEE Trans. Signal Processing.*
[10] H. Cox, A. Pezeshki, L. L. Scharf, M. Lundberg, and H. Lai, "Multi-rank adaptive beamforming with linear and quadratic constraints," in *Conf. Rec. Thirty-Ninth Asilomar Conf. Signals, Syst., Comput.,* Pacific Grove, CA, Oct. 30-Nov. 2, 2005.